Microscopic mechanisms of magnetic transitions in chain polymeric copper(II) complexes with nitronyl nitroxide radicals

E. M. Zueva, E. R. Ryabykh, and An. M. Kuznetsov*

Kazan State Technological University,
68 ul. K. Marksa, 420015 Kazan, Russian Federation.
Fax: +7 (843) 238 5694. E-mail: zueva_ekaterina@mail.ru

Parameters of exchange interactions in heterospin chain polymeric complexes of $Cu(hfac)_2$ (hfac is hexafluoroacetylacetonate anion) with pyrazolyl-substituted nitronyl nitroxides L^R (R = Me, Et, Pr, Bu) were estimated using quantum chemical computational methods. The magnetic properties of the considered chain polymeric complexes can be described within the framework of the model of isolated exchange clusters. Experimental data on the structural dynamics of chains polymeric with "head-to-tail" (R = Me) and "head-to-head" (R = Et, Pr, Bu) motifs are discussed in the context of the concept of gradual phase transitions. Based on the analysis performed, a hypothesis of microscopic mechanisms of magnetic transitions in crystals of this type of compounds was proposed.

Key words: metal hexafluoroacetylacetonates, nitroxide radicals, spin transitions, quantum chemical calculations, density functional theory, exchange coupling, broken symmetry method.

Recently,[1—6] a family of heterospin complexes $Cu(hfac)_2$ (hfac is hexafluoroacetylacetonate anion) with pyrazolyl-substituted nitronyl nitroxides L^R (R = Me, Et, Pr, Bu) has been discovered. In the solid phase, these compounds can undergo a reversible transition from the high-spin to the low-spin state when exposed to repeated cooling—heating cycles.

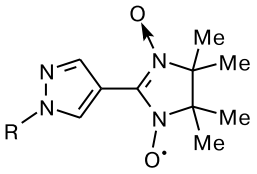

L^R

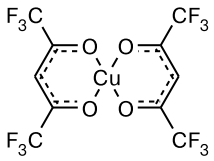

$Cu(hfac)_2$

Crystals of these complexes have a chain polymeric structure due to a bidentate bridged coordination of paramagnetic ligands L^R through the imine nitrogen atom and the nitroxide oxygen atom. Chains can have a "head-to-tail" or a "head-to-head" motif. A unique feature of these compounds is that a structural rearrangement of the crystal, which causes the effective magnetic moment to change (sometimes, in a jumpwise manner), occurs at relatively high temperatures (130—230 K). High mechanical stability of crystals of the complexes in the temperature variation and on crossing the magnetic transition region is also unusual.

Earlier,[1—6] it has been assumed that the observed temperature dependences of the effective magnetic moment are mainly due to reversible structural rearrangements of the coordination polyhedra in the CuO_5N sites (a "head-to-tail" motif) or CuO_6 sites (a "head-to-head" motif) and that they can be described within the framework of the model of isolated exchange clusters. In the present work, using modern computational methods of quantum chemistry, we have substantiated the assumption of the applicability of the model of isolated exchange clusters to the description of the magnetic properties of chain polymeric complexes of $Cu(hfac)_2L^R$ and proposed a hypothesis of microscopic mechanisms of magnetic transitions in crystals of this type of compounds.

Calculation Procedure

All calculations were carried out within the framework of the density functional theory using the B3LYP hybrid exchange-correlation functional,[7—9] the spin-unrestricted SCF procedure (UB3LYP), and the GAUSSIAN-98 program package.[10]

The exchange parameters of the Heisenberg—Dirac—van Vleck spin Hamiltonian, which describe interactions between localized electron spins, were estimated by the broken symmetry method[11—14] (for discussion, see Refs 15—21). This method establishes a one-to-one correspondence between diagonal elements of the Heisenberg—Dirac—van Vleck spin Hamiltonian matrix computed in products of single-center spin functions and diagonal elements of the electron Hamiltonian matrix computed in single-determinant wave functions (WF), which represent the highest-spin (HS) state and the so-called broken-symmetry (BS) states with different occupation of magnetic spin orbitals. It should be noted that, owing to spin "contamination" and nonorthogonality of the computed HS and BS determinants, this correspondence holds only approximately.[21]

Published in Russian in *Izvestiya Akademii Nauk. Seriya Khimicheskaya,* No. 8, pp. 1605—1613, August, 2009.

1066-5285/09/5808-1654

Single-determinant WF representing different spin configurations were calculated using the rigorous convergence criterion (parameter scf = "tight"), which ensures sufficiently well-converged values of the HS- and BS-state energies. For all states, the stability analysis[22] for the solution obtained (parameter stable = "opt") was performed.

Calculations were carried out with the TZVP/SVP basis set,[23,24] which proved itself in estimating the exchange parameters within the framework of the UB3LYP-BS computational procedure.[16,19,21,25–34] This basis set includes a triple-zeta split-valence basis set augmented with a polarization function (TZVP) for the copper, oxygen, and nitrogen atoms and a double-zeta split-valence basis set augmented with a polarization function (SVP) for the carbon, fluorine, and hydrogen atoms.

Results and Discussion

A structural phase transition requires the overcoming of a barrier between the Gibbs free energy minima corresponding to stable polymorphs of the crystal in the vicinity of the transition. The barrier significantly decreases if structural rearrangement occurs gradually by nucleation and successive growth of domains of the new phase. In such cases, the polymorphous transformation involves a sequence of metastable structures with broken translational symmetry, which undergo transitions into one another due to small-scale thermal fluctuations whose probability is rather high.

This microscopic phase transition mechanism is characteristic of the so-called Jahn—Teller crystals containing labile coordination sites capable of changing their shape under weak thermal excitations. Therefore, it is reasonable to admit[6] that this general concept of gradual phase transitions is also applicable to typical representatives of the Jahn—Teller crystals, *viz.*, chain polymeric complexes of $Cu(hfac)_2L^R$. Considering this admission as a working hypothesis, we will analyze the available experimental data on the structural dynamics of polymer chains with the "head-to-tail" and "head-to-head" motifs and try to relate them to the observed temperature dependences of the effective magnetic moment based on the results of quantum chemical calculations of exchange parameters of the Heisenberg—Dirac—van Vleck spin Hamiltonian carried out in the present work.

Polymer chains with the "head-to-tail" motif. We will consider structural and magnetic transitions in the polymer chains with the "head-to-tail" motif taking the triclinic modification of $Cu(hfac)_2L^{Me}$ as an example. The molecular structure of chains in this compound is schematically presented in Fig. 1. The repeating unit of the chain is shown below.

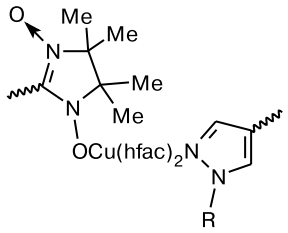

Neighboring repeating units form structurally equivalent dyads representing one period of the chain in the crystal. Each dyad comprises two crystallographically independent CuO_5N coordination sites containing the $Cu^{2+}—O^{\cdot}—N$ exchange clusters.

The Cu^{2+} ion belongs to the Jahn—Teller ions having a degenerate ground electronic state in octahedral ligand field. In this connection, a highly symmetric (O_h) geometric configuration of isolated copper(II) complexes is unstable and corresponds to the vertices of equal-height potential barriers between three equivalent minima corresponding to an octahedron extended or contracted along one of the three fourfold axes. The barrier height is determined by weak vibronic coupling, which includes the dependence of electronic energy on the vibrational coordinates of atomic nuclei, and is usually very small. Because of this, a characteristic feature of isolated copper(II) complexes is the dynamic Jahn—Teller effect, *i.e.*, the formation of coupled electronic-vibrational states, which leads to tunnel splitting of vibrational levels.[35,36]

The coordination sites formed by the Cu^{2+} ion in molecular or chain polymeric crystals, succeed the stable geometry of isolated complexes. However, local potential barriers between the stable configurations of sites in the crystal are always higher than in isolated complex because they are determined by not only weak vibronic coupling, but also external forces acting on a given site (crystal field effect). Therefore, the dynamic Jahn—Teller effect in solids is rarely observed. Typically, transitions of coordination sites from one stable form to another are induced by random vibrational excitations, which can be either local or concerted in character.

According to X-ray diffraction data,[4] stable geometric configurations of the CuO_5N coordination sites in chains with the "head-to-tail" motif have the shape of an extended octahedron and can be divided into two types depending on the position of the long axis in the polyhedron. One type of sites has the $N_L—Cu—O_L$ long axis; the $Cu^{2+}—O^{\cdot}—N$ heterospin cluster is characterized by predominance of ferromagnetic exchange typical at $Cu—O_L$ bond lengths of ~2.4 Å or more[1,2] (hereafter, F-sites). The other type of sites has the $O_{hfac}(1)—Cu—O_{hfac}(3)$ long axis (see Fig. 1). In these sites, the $Cu—O_L$ distance is shortened to ~2.0 Å, which leads to significant stabilization of antiferromagnetic spin ordering and to inversion of spin levels in the exchange cluster (hereafter, AF-sites). The second possible AF-configuration with the $O_{hfac}(2)—Cu—O_{hfac}(4)$ long axis in the stable structural modifications of the $Cu(hfac)_2L^{Me}$ crystal is not realized. Emphasize that the types of the coordination sites and the order of their appearance in the chain depend on many factors and are by and large

controlled by the thermodynamic potential of the whole crystal.

Isotropic exchange in Cu^{2+}—O˙—N two-center clusters is described by the model spin Hamiltonian

$$H = -2J\mathbf{S}_{Cu}\mathbf{S}_{L}. \quad (1)$$

This Hamiltonian ignores interchain and cluster—cluster interactions and depends on a single parameter J, which describes the exchange interaction between the spins localized on the Cu^{2+} ion and on the nitronyl nitroxide fragment. The eigenvalues of the spin Hamiltonian (1), which determine the relative positions of the spin levels of the two-center exchange cluster, are given by

$$^{3}E = -(1/2)J,\ ^{1}E = (3/2)J. \quad (2)$$

The parameter J was evaluated as follows:

$$J = -(E_{HS} - E_{BS}), \quad (3)$$

where E_{HS} and E_{BS} are the energies of the HS- and BS-states, which were calculated for the $\{L^{Me}—Cu(hfac)_2—L^{Me}\}$ chain fragment using the X-ray diffraction data obtained at temperatures above and below the structural phase transition temperature (T_{PT}).

Similar calculations were also carried out for the $\{L^{Me}—Cu(hfac)_2—L^{Me}–Cu(hfac)_2—L^{Me}\}$ chain fragment using the model spin Hamiltonian, which includes all possible pair interactions in the O˙—N···Cu^{2+}—O˙——N···Cu^{2+}—O˙—N exchange cluster. It was shown that the exchange parameters of the Cu^{2+}–O˙–N fragments of the five-center cluster are nearly equal to those of the two-center clusters calculated using expression (3), while other pair interactions are negligible. Clearly, the Cu^{2+}—O˙—N exchange clusters are isolated from one another in the polymer chains of the $Cu(hfac)_2L^{Me}$ complex.

The bond lengths and the exchange parameters of the coordination sites of the $Cu(hfac)_2L^{Me}$ crystal are listed in Table 1. The values in parentheses refer to the exchange parameters estimated within the framework of the Yamaguchi algorithm,[18] which to some extent includes the nonorthogonality of the magnetic orbitals in the WF of the BS-states. Note that for the complexes in question, this correction is significant only for the AF-sites.

From the data of Table 1 it follows that the structural period of the chain in the high-temperature phase ($T > T_{PT}$) of the $Cu(hfac)_2L^{Me}$ crystal comprises two F-sites characterized by close geometric parameters and small positive J values. In these coordination sites, the energy gap between the ground (triplet) and excited (singlet) spin states of the exchange cluster is narrow; as a consequence, the room-temperature population of the singlet state is high. As the temperature decreases, the population of this state also decreases, which manifests itself in the experimentally observed gradual increase in μ_{eff} in the high-temperature region. In the low-temperature phase ($T < T_{PT}$), one site of the structural period of the chain has the AF-configuration (see Table 1). The type of 50% of sites of the crystal is changed concertedly at the phase transition temperature, which predetermines a jumpwise decrease or increase in the effective magnetic moment on cooling or heating, respectively.* The fact that the other 50% of sites in the low-temperature phase remain in the F-configuration provides an explanation for a gradual increase in μ_{eff} on cooling.

The molar magnetic susceptibility and the effective magnetic moment calculated per $\{Cu(hfac)_2L^{Me}\}$ fragment are given by the following expressions (ignoring diamagnetic contribution):

$$\chi = 0.5\chi_1 + 0.5\chi_2,$$

$$\mu_{eff} = \sqrt{3kT\chi/(N\mu_B^2)}.$$

Here χ_1 and χ_2 are the molar magnetic susceptibilities of the exchange clusters in the coordination sites:

$$\chi_i = \frac{N\mu_B^2 g^2}{3kT}\frac{6\exp[-{}^{3}E/(kT)]}{\exp[-{}^{1}E/(kT)] + 3\exp[-{}^{3}E/(kT)]} + N\alpha,$$

$$g = (g_{Cu} + g_L)/2,$$

where N is the Avogadro constant, μ_B is the Bohr magneton, k is the Boltzman constant, ^{3}E and ^{1}E are the eigenvalues of the spin Hamiltonian (1) calculated using

* The μ_{eff} jump for $Cu(hfac)_2L^{Me}$ is observed at 141 (cooling) and 146 K (heating).

Table 1. Bond lengths (d) and exchange parameters (J) in coordination sites of $Cu(hfac)_2L^{Me}$ crystal

T/K	Central atom	d/Å			J/cm^{-1}
		Cu—N_L/Cu—O_L	Cu—$O_{hfac}(4)$/Cu—$O_{hfac}(2)$	Cu—$O_{hfac}(3)$/Cu—$O_{hfac}(1)$	
140	Cu(1)	2.014/1.992	1.981/2.004	2.259/2.289	−958 (−873)
	Cu(2)	2.336/2.449	1.976/1.966	1.937/1.935	16 (16)
293	Cu(1)	2.298/2.507	1.937/1.959	1.948/1.968	31 (31)
	Cu(2)	2.323/2.508	1.941/1.964	1.930/1.947	15 (15)

Note. The values in parentheses refer to the exchange parameters calculated within the framework of the Yamaguchi algorithm.[18]

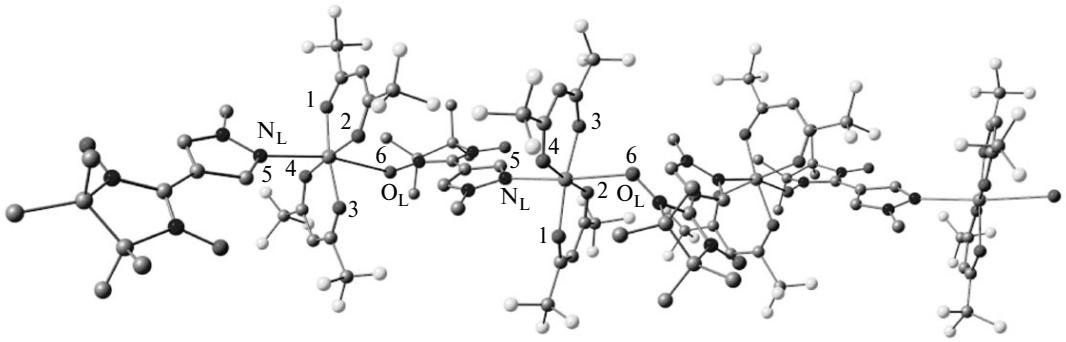

Fig. 1. Polymer chain with the "head-to-tail" motif.*

expressions (2), and $N\alpha$ is the correction for temperature-independent paramagnetism. When constructing the temperature dependences of the magnetic properties of the $Cu(hfac)_2L^{Me}$ complex, the F-sites can be described using a single parameter J_F. In this case, $\chi = \chi_F$ for the high-temperature phase ($J_1 = J_2 = J_F$) and $\chi = 0.5\chi_{AF} + 0.5\chi_F$ for the low-temperature phase ($J_1 = J_{AF}$, $J_2 = J_F$). One can show with ease that the theoretical curve $\mu_{eff}(T)$ plotted using the calculated J values (see Table 1) reproduces the character of the experimental dependence in the whole temperature interval. The optimum J_F and J_{AF} values for the description of the magnetic properties of the $Cu(hfac)_2L^{Me}$ complex (and the g-factors of the paramagnetic centers) can be determined from the results of magnetochemical measurements using the expressions given above.

Polymer chains with the "head-to-head" motif. The molecular structure of chains of the complexes $Cu(hfac)_2L^{Bu} \cdot 0.5C_6H_{14}$, $Cu(hfac)_2L^{Pr}$, and $Cu(hfac)_2L^{Et}$ is schematically shown in Fig. 2. The repeating unit of the chain comprises two sites, CuO_6 and CuO_4N_2 (see below).

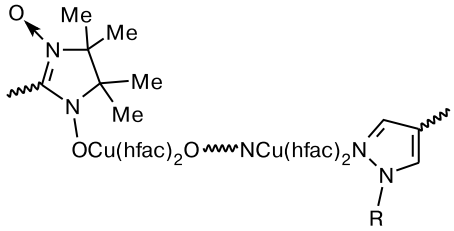

The CuO_6 site contains the N—·O—Cu^{2+}—O·—N exchange cluster; the CuO_4N_2 site has a single unpaired electron localized on the metal center. Clearly, the character of the temperature dependence of the effective magnetic moment is determined by the changes in the geometry of the CuO_6 sites in which exchange interactions between electron spins occur.

Isotropic exchange in the N—·O—Cu^{2+}—O·—N three-center clusters is described by the following model spin Hamiltonian:

$$H = -2J(\mathbf{S}_L\mathbf{S}_{Cu} + \mathbf{S}_{Cu}\mathbf{S}_L) - 2J'\mathbf{S}_L\mathbf{S}_L. \quad (4)$$

In writing the expression for the Heisenberg—Dirac—van Vleck spin Hamiltonian, we admitted that the

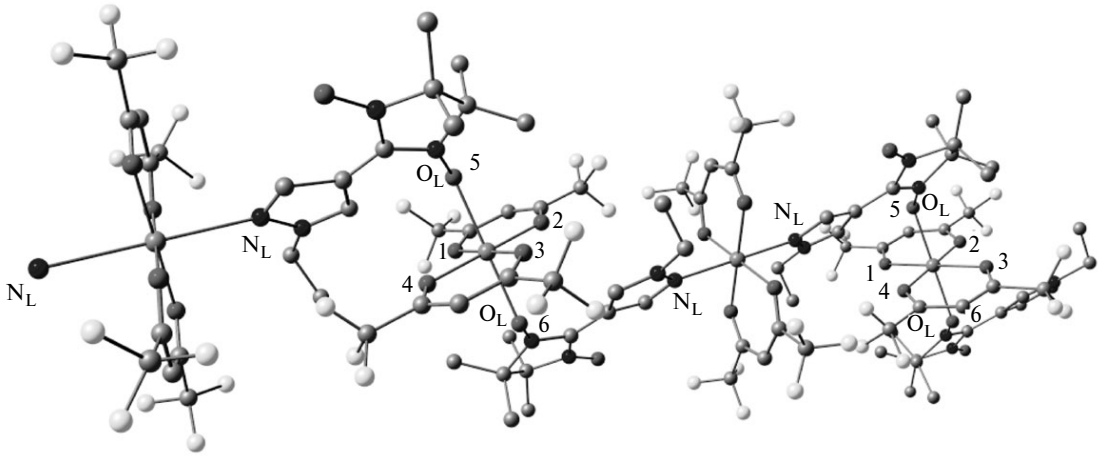

Fig. 2. Polymer chain with the "head-to-head" motif.

* Figures 1 and 2 are available in full color in the on-line version of the journal (http://www.springerlink.com).

exchange between the Cu^{2+} ion and the nitroxyl group of any of the two coordinated radicals can be described using a single parameter. The eigenvalues of the spin Hamiltonian (4), which determine the relative positions of the spin levels of the three-center exchange cluster, are as follows:

$$^4E = -J - (1/2)J', \; ^2E_1 = (3/2)J', \; ^2E_2 = 2J - (1/2)J'. \quad (5)$$

The parameters J and J' were evaluated using the following expressions:

$$E_{HS} - E_{BS1} = -J - J', \quad (6a)$$

$$E_{HS} - E_{BS2} = -2J, \quad (6b)$$

where E_{HS}, E_{BS1}, and E_{BS2} are the energies of the HS- and BS-states calculated for the $\{L^R—Cu(hfac)_2—L^R\}$ chain fragment using X-ray diffraction data for the stable geometric configurations of the CuO_6 sites.

Similar calculations were carried out for the $\{L^R—Cu(hfac)_2—L^R—Cu(hfac)_2—L^R\}$ chain fragment containing the N—·O—Cu^{2+}—O·—N···Cu^{2+}···N—·O exchange cluster. From the results obtained it follows that the exchange parameters of the N—·O—Cu^{2+}—O·—N fragment of the five-center cluster are nearly equal to those obtained for the three-center cluster using expressions (6), while the remaining pair interactions are negligible. Apparently, in the chains with the "head-to-head" motif the exchange clusters N—·O—Cu^{2+}—O·—N of the CuO_6 sites do not interact with the Cu^{2+} ions of neighboring CuO_4N_2 sites.

According to X-ray diffraction data (see Ref. 4), stable geometric configurations of the CuO_6 sites also have the shape of an extended octahedron and belong to the F- and AF-types. In the F-sites, the long axis is O_L—Cu—O_L (Cu—O_L ~2.3 Å) and ferromagnetic exchange stabilizing the quartet spin state dominates in the N—·O—Cu^{2+}——O·—N exchange cluster. The AF-sites with the $O_{hfac}(1)$—Cu—$O_{hfac}(3)$ long axis are characterized by short Cu—O_L distances (~2.0 Å) and a large negative J value. The change in the character of exchange upon shortening of the Cu—O_L distances leads to inversion of the spin levels in the exchange cluster and to a considerable increase in the energy intervals between them.

Consider structural rearrangements of the CuO_6 sites in the $Cu(hfac)_2L^{Bu}\cdot 0.5C_6H_{14}$, $Cu(hfac)_2L^{Pr}$, and $Cu(hfac)_2L^{Et}$ crystals in more detail. The crystal structure of the $Cu(hfac)_2L^{Bu}\cdot 0.5C_6H_{14}$ complex was determined at twelve temperatures (Table 2). In solving the structure of the high-temperature phase, the CuO_6 sites were assumed to be structurally equivalent. At room temperature, the crystallographic geometry of the CuO_6 sites formally corresponds to the F-configuration, *viz.*, the Cu—O_L distances are rather long (2.311 Å), while the Cu—O_{hfac} distances are much shorter (1.971—1.984 Å). Calculations of the exchange parameters using expressions (6) give the values characteristic of the F-sites, *viz.*, $J = 44$ cm^{-1} and $J' = -5$ cm^{-1}. Would the coordination sites in the high-temperature phase of the crystal preserve their geometric configuration on cooling, one should expect a gradual increase in the effective magnetic

Table 2. Bond lengths (d) in CuO_6 sites (central symmetry) and weight fractions (w) of AF-sites in $Cu(hfac)_2L^{Bu}\cdot 0.5C_6H_{14}$ crystal

T/K	w	Central atom	d/Å		
			Cu—O_L	Cu—$O_{hfac}(2)$	Cu—$O_{hfac}(1)$
110	0.5	Cu(1)	2.344	1.958	1.964
		Cu(2)	1.995	2.031	2.228
120	0.5	Cu(1)	2.342	1.956	1.965
		Cu(2)	1.994	2.028	2.231
130	0.5	Cu(1)	2.340	1.955	1.967
		Cu(2)	1.996	2.026	2.229
140	0.5	Cu(1)	2.341	1.955	1.969
		Cu(2)	2.000	2.021	2.227
150	0.5	Cu(1)	2.337	1.955	1.970
		Cu(2)	2.008	2.022	2.217
163	0.254	Cu	2.248 (2.255)	1.974 (1.977)	2.022 (2.031)
167	0.252	Cu	2.250 (2.256)	1.976 (1.976)	2.023 (2.031)
171	0.250	Cu	2.251 (2.257)	1.975 (1.976)	2.023 (2.030)
186	0.223	Cu	2.259 (2.266)	1.973 (1.974)	2.014 (2.023)
200	0.207	Cu	2.265 (2.272)	1.973 (1.973)	2.010 (2.019)
240	0.147	Cu	2.287 (2.293)	1.971 (1.969)	1.995 (2.003)
295	0.090	Cu	2.311 (2.313)	1.971 (1.965)	1.984 (1.988)

Note. Here and in Tables 3 and 4 the values in parentheses are the bond lengths calculated using expression (7).

moment on cooling to 164 K (temperature at which μ_{eff} abruptly decreases*). However, a gradual decrease in the effective magnetic moment on cooling is observed in the high-temperature region. Probably, this behavior of the high-temperature phase of the crystal is due to the fact that local thermal fluctuations on cooling cause certain F-sites to undergo transitions to the AF-configuration, *i.e.*, the number of AF-sites in the polymer chains gradually increases. According to X-ray diffraction data, the high-temperature phase of the crystal does undergo structural rearrangements as the temperature changes. For instance, in the CuO_6 sites the $Cu—O_L$ distances are gradually shortened (2.311 → 2.248 Å), whereas the $Cu—O_{hfac}$ distances along the $O_{hfac}(1)—Cu—O_{hfac}(3)$ axis are lengthened (1.984 → 2.022 Å) on cooling to 163 K. Clearly, these geometric parameters of the coordination sites correspond to none of the stable geometric configurations. The crystallographic parameters of the CuO_6 sites in the high-temperature phase can be described as follows:

$$d = wd_{AF} + (1 - w)d_F, \qquad (7)$$

where d_{AF} and d_F are the parameters of stable geometric configurations and w and $1 - w$ are respectively the weight fractions of the AF- and F-sites at the specified temperature. It cannot be ruled out that a small fraction of the CuO_6 sites is in the AF-configuration already at room temperature. On cooling, the weight fraction of the AF-sites gradually increases.

The structure of the low-temperature phase was determined at 150, 140, 130, 120, and 110 K. In solving the structure of the low-temperature phase, the chain period was represented by a fragment comprising two neighboring repeating units, each containing the CuO_6 and CuO_4N_2 sites (see above). According to X-ray diffraction data, the geometric parameters of the CuO_6 sites of the chain period remain almost unchanged in the temperature interval 150—110 K (see Table 2). Therefore, the CuO_6 sites in the crystal retain their geometric configuration as temperature varies within these limits. Clearly, at low temperatures the crystal adopts a stable structural modification possessing translational symmetry. In this case, the crystallographic geometry of the CuO_6 sites corresponds to stable configurations. From the data of Table 2 it follows that one CuO_6 site of the chain period is in the F-configuration ($Cu—O_L$ ~2.34 Å, $Cu—O_{hfac}(1)$ ~1.97 Å, $Cu—O_{hfac}(2)$ ~1.96 Å), while the other CuO_6 site is in the AF-configuration ($Cu—O_L$ ~2.00 Å, $Cu—O_{hfac}(1)$ ~2.23 Å, $Cu—O_{hfac}(2)$ ~2.03 Å). We used the X-ray diffraction data (110 K) to evaluate the exchange parameters of stable geometric configurations of the CuO_6 sites and obtained $J_F = 41$ (41) cm^{-1}, $J'_F = -5$ (−5) cm^{-1}; $J_{AF} = -834$ (−767) cm^{-1}, and $J'_{AF} = -23$ (−22) cm^{-1} (hereafter numbers in parentheses are the values obtained within the framework of the Yamaguchi algorithm[18]).

Taking the bond lengths determined by low-temperature X-ray analysis as d_{AF} and d_F, one can estimate the weight fractions of the AF-sites in the high-temperature phase by solving the redundant system of equations (7) by the least squares method. The w values thus obtained are listed in Table 2. Our estimates are as follows: at 295 K, 9% of the CuO_6 sites are in the AF-configuration; at 163 K, the weight fraction of the AF-sites increases to 25.4%. Clearly, gradual increase in the number of the AF-sites in the high-temperature phase of the crystal predetermines a gradual decrease in the effective magnetic moment on cooling. At a certain critical temperature (164 K), μ_{eff} abruptly decreases. In the low-temperature phase ($T < 150$ K), polymer chains possess translational symmetry, w takes a value of 0.5 and is temperature independent. The fact that 50% of CuO_6 sites in the low-temperature phase are in the F-configuration provides an explanation for the gradual increase in the effective magnetic moment on further cooling.

The molar magnetic susceptibility and the effective magnetic moment per $\{Cu(hfac)_2L^{Bu} \cdot 0.5C_6H_{14}\}$ fragment are given by (ignoring diamagnetic contribution)

$$\chi = 0.5\chi_{ex} + 0.5\chi_{mono},$$

$$\mu_{eff} = \sqrt{3kT\chi/(N\mu_B^2)},$$

where χ_{mono} is the molar magnetic susceptibility of Cu^{2+} ions in the CuO_4N_2 sites ($S = 1/2$) and χ_{ex} is the molar magnetic susceptibility of the $N—{}^{\cdot}O—Cu^{2+}—O^{\cdot}—N$ exchange clusters in the CuO_6 sites with allowance for the weight fractions of the AF- and F-sites:

$$\chi_{mono} = [N\mu_B^2 g_{Cu}^2/(3kT)]S(S + 1) + N\alpha,$$

$$\chi_{ex} = w\chi_{AF} + (1 - w)\chi_F.$$

The expressions for the molar magnetic susceptibilities χ_{AF} and χ_F of the exchange clusters in the AF- and F-sites have the form:

$$\chi_i = \frac{N\mu_B^2}{3kT} \frac{1.5g_A^2 e^{-\frac{^2E_1}{kT}} + 1.5g_B^2 e^{-\frac{^2E_2}{kT}} + 15g_C^2 e^{-\frac{^4E}{kT}}}{2e^{-\frac{^2E_1}{kT}} + 2e^{-\frac{^2E_2}{kT}} + 4e^{-\frac{^4E}{kT}}} + N\alpha,$$

$$g_A = g_{Cu},\ g_B = (4g_L - g_{Cu})/3,\ g_C = (2g_L + g_{Cu})/3.$$

Here ^4E, $^2E_1$, and $^2E_2$ are the eigenvalues of the spin Hamiltonian (4), which are calculated using relationships (5). When constructing the temperature dependences of the magnetic properties of the $Cu(hfac)_2L^{Bu} \cdot 0.5C_6H_{14}$ complex, one should know the $w(T)$ dependence in the

* The μ_{eff} jump for $Cu(hfac)_2L^{Bu} \cdot 0.5C_6H_{14}$ is observed at 161±3 K.

Table 3. Bond lengths (d) in the CuO_6 sites (central symmetry) and the weight fractions (w) of the AF-sites in $Cu(hfac)_2L^{Pr}$ crystal

T/K	w	Central atom	d/Å		
			Cu—O_L	Cu—$O_{hfac}(2)$	Cu—$O_{hfac}(1)$
50	1.0	Cu	1.993	1.952	2.272
115	0.960	Cu(1)	2.023	1.962	2.280
		Cu(2)	2.022 (2.007)	1.967 (1.952)	2.277 (2.260)
145	0.875	Cu(1)	2.047	1.963	2.236
		Cu(2)	2.044 (2.037)	1.959 (1.953)	2.242 (2.233)
175	0.745	Cu(1)	2.090	1.965	2.191
		Cu(2)	2.083 (2.083)	1.958 (1.954)	2.194 (2.193)
195	0.616	Cu(1)	2.114	1.962	2.139
		Cu(2)	2.115 (2.128)	1.955 (1.954)	2.139 (2.154)
205	0.565	Cu(1)	2.140	1.965	2.132
		Cu(2)	2.140 (2.146)	1.965 (1.955)	2.132 (2.138)
215	0.513	Cu(1)	2.158	1.960	2.111
		Cu(2)	2.154 (2.164)	1.956 (1.955)	2.111 (2.122)
220	0.472	Cu(1)	2.171	1.963	2.099
		Cu(2)	2.169 (2.178)	1.957 (1.955)	2.099 (2.109)
229	0.324	Cu	2.217 (2.230)	1.957 (1.956)	2.049 (2.064)
232	0.298	Cu	2.231 (2.239)	1.958 (1.956)	2.046 (2.056)
240	0.218	Cu	2.256 (2.267)	1.960 (1.957)	2.018 (2.031)
293	0.057	Cu	2.318 (2.324)	1.955 (1.958)	1.975 (1.982)

high-temperature region. The w values we have obtained and the exchange parameters of the F- and AF-sites allow one to correctly describe the character of the experimental $\mu_{eff}(T)$ dependence both in the high- and low-temperature regions. The optimum values of J_F, J'_F, J_{AF}, and J'_{AF} (as well as the g-factors of the paramagnetic centers) can be estimated from the data of magnetochemical experiment for the low-temperature phase ($T < 150$ K) using the expressions given above and $w = 0.5$. The values thus obtained will make it possible to determine the shape of the $w(T)$ dependence in the high-temperature region from the experimental $\chi(T)$ dependence.

Table 3 lists the X-ray diffraction data for the $Cu(hfac)_2L^{Pr}$ complex. Formally, the room-temperature geometric parameters of the CuO_6 sites in $Cu(hfac)_2L^{Pr}$ correspond to the F-configuration. Cooling causes a gradual shortening of the Cu—O_L distances and elongation of the Cu—O_{hfac} distances along the $O_{hfac}(1)$—Cu—$O_{hfac}(3)$ axis (see Table 3); this indicates accumulation of AF-sites in polymer chains. At rather low temperatures, the crystal adopts a stable structural modification in which the CuO_6 sites have the AF-configuration (see Table 3). Our estimates gave $J_{AF} = -825$ (-759) cm^{-1} and $J'_{AF} = -28$ (-27) cm^{-1}.

The weight fractions of the AF-sites calculated by solving the redundant system of equations (7) by the least squares method are listed in Table 3. When estimating the w values, we suggested the geometric parameters of the F-configuration of the CuO_6 sites to be equal to those of the F-sites in $Cu(hfac)_2L^{Bu} \cdot 0.5C_6H_{14}$ (see Table 2, 110 K). Our estimates show that the weight fraction of the AF-sites gradually increases on cooling. As should be expected, a gradual decrease in the effective magnetic moment in the high-temperature region ($T > \sim 240$ K) is observed for this compound on cooling. A noticeable decrease in μ_{eff} is observed in a broad temperature interval from about 240 to nearly 140 K. Further cooling leads to a gradual decrease in the effective magnetic moment. The theoretical curve $\mu_{eff}(T)$ plotted using the weight fractions and the exchange parameters of the AF- and F-sites* calculated in the present work reproduces the character of the experimental dependence in the whole temperature range studied.

The structure and magnetic properties of the $Cu(hfac)_2L^{Et}$ complex deserve a more thorough consideration. This compound has quite an unusual $\mu_{eff}(T)$ dependence. Namely, the effective magnetic moment decreases on cooling to 220 K, increases jumpwise at 220 K, and then increases as the temperature decreases further. The X-ray diffraction data for $Cu(hfac)_2L^{Et}$ are listed in Table 4. The structure was solved assuming that all CuO_6 sites are structurally equivalent. From the data of Table 4 it follows that at room temperature a noticeable proportion of CuO_6 sites is in the AF-configuration and that the weight fraction of the AF-sites increases on cooling to 241 K. In the temperature interval 241—221 K, the CuO_6

* The exchange parameters of the F-configuration of the CuO_6 sites can be set equal to those of the F-sites in $Cu(hfac)_2L^{Bu} \cdot 0.5C_6H_{14}$.

Table 4. Bond lengths (d) in the CuO_6 sites (central symmetry) and the weight fractions (w) of the AF-sites in $Cu(hfac)_2L^{Et}$ crystal

T/K	w	d/Å		
		Cu—O_L	Cu—$O_{hfac}(2)$	Cu—$O_{hfac}(1)$
30	0.0	2.292	1.947	1.956
115	0.066	2.281 (2.272)	1.958 (1.947)	1.985 (1.977)
188	0.138	2.260 (2.251)	1.960 (1.948)	2.008 (2.000)
208	0.141	2.260 (2.250)	1.961 (1.948)	2.010 (2.001)
215	0.165	2.249 (2.243)	1.960 (1.948)	2.014 (2.008)
218	0.190	2.242 (2.235)	1.961 (1.948)	2.022 (2.016)
221	0.354	2.176 (2.186)	1.956 (1.949)	2.058 (2.068)
229	0.381	2.175 (2.178)	1.969 (1.949)	2.073 (2.076)
241	0.356	2.183 (2.186)	1.968 (1.949)	2.066 (2.068)
293	0.209	2.237 (2.230)	1.965 (1.948)	2.029 (2.022)

sites probably retain their geometric configuration. At 220 K, the weight fraction of the AF-sites abruptly decreases. Further cooling is also accompanied by transition of the CuO_6 sites from the AF- to the F-configuration; however, the weight fraction of the AF-sites decreases gradually. At rather low temperatures, the crystal probably adopts a stable structural modification with the CuO_6 sites in the F-configuration. In this case, the X-ray diffraction data obtained at 30 K correspond to this configuration (see Table 4). An interesting feature of the F-sites in $Cu(hfac)_2L^{Et}$ is relatively short Cu—O_L distances (2.292 Å). Our estimates gave $J_F = 47$ (47) cm^{-1} and $J'_F = -7$ (-7) cm^{-1}.

The w values calculated by solving the redundant system of equations (7) by the least squares method are listed in Table 4. When estimating the w values, we considered the geometric parameters of the AF-configuration of the CuO_6 sites to be equal to those of $Cu(hfac)_2L^{Pr}$ (see Table 3, 50 K). The w values we have obtained and the exchange parameters of the F- and AF-sites* allow one to correctly describe the character of the experimental $\mu_{eff}(T)$ dependence both in the high- and low-temperature regions. In the temperature interval 241—221 K, the crystal probably adopts a stable structural modification in which the chain period can be represented by a fragment comprising three repeating units. Our estimates show that one CuO_6 site of the structural period of the chain is in the AF-configuration, while the other two CuO_6 sites have the F-configuration.

Summing up, our study of the structure and magnetic properties of chain polymeric complexes $Cu(hfac)_2$ with pyrazolyl-substituted nitronyl nitroxides showed that the polymer chains with the "head-to-tail" motif comprising the CuO_5N sites are characterized by high cooperativity, *viz.*, transitions of the coordination sites from one stable configuration to the other occur concertedly. Contrary to this, polymer chains with the "head-to-head" motif comprise alternating CuO_6 and CuO_4N_2 sites, which significantly lowers the cooperativity within the chain. As a result, the phase transition occurs gradually and involves a sequence of metastable structures with broken translational symmetry.

* The exchange parameters of the AF-configuration of the CuO_6 sites can be set equal to those of the AF-sites in $Cu(hfac)_2L^{Pr}$.

The authors express their gratitude to V. I. Ovcharenko and G. V. Romanenko for helpful discussion, valuable comments, and access to X-ray diffraction data.

References

1. V. I. Ovcharenko, S. V. Fokin, G. V. Romanenko, Yu. G. Shvedenkov, V. N. Ikorskii, E. V. Tret´yakov, S. F. Vasilevskii, *Zh. Struktur. Khim.*, 2002, **43**, 163 [*Russ. J. Struct. Chem.* (*Engl. Transl.*), 2002, **43**, 153].
2. V. I. Ovcharenko, S. V. Fokin, G. V. Romanenko, V. N. Ikorskii, E. V. Tretyakov, S. V. Vasilevsky, R. Z. Sagdeev, *Mol. Phys.*, 2002, **100**, 1107.
3. P. Rey, V. I. Ovcharenko, in *Magnetism: Molecules to Materials IV*, Eds J. S. Miller, M. Drillon, Wiley-VCH, Weinheim, 2003, 41.
4. V. I. Ovcharenko, K. Yu. Maryunina, S. V. Fokin, E. V. Tret´yakov, G. V. Romanenko, V. N. Ikorskii, *Izv. Akad. Nauk, Ser. Khim.*, 2004, 2304 [*Russ. Chem. Bull., Int. Ed.*, 2004, **53**, 2406].
5. S. Fokin, V. Ovcharenko, G. Romanenko, V. Ikorskii, *Inorg. Chem.*, 2004, **43**, 969.
6. V. I. Ovcharenko, G. V. Romanenko, K. Yu. Maryunina, A. S. Bogomyakov, E. V. Gorelik, *Inorg. Chem.*, 2008, **47**, 9537.
7. A. D. Becke, *J. Chem. Phys.*, 1993, **98**, 5648.
8. A. D. Becke, *Phys. Rev. A*, 1988, **38**, 3098.
9. C. Lee, W. Yang, R. G. Parr, *Phys. Rev. B*, 1988, **37**, 785.
10. M. J. Frisch, G. W. Trucks, H. B. Schlegel, G. E. Scuseria, M. A. Robb, J. R. Cheeseman, J. A. Montgomery, Jr., T. Vreven, K. N. Kudin, J. C. Burant, J. M. Millam, S. S. Iyengar, J. Tomasi, V. Barone, B. Mennucci, M. Cossi, G. Scalmani, N. Rega, G. A. Petersson, H. Nakatsuji, M. Hada, M. Ehara, K. Toyota, R. Fukuda, J. Hasegawa, M. Ishida, T. Nakajima, Y. Honda, O. Kitao, H. Nakai, M. Klene, X. Li, J. E. Knox, H. P. Hratchian, J. B. Cross, V. Bakken, C. Adamo, J. Jaramillo, R. Gomperts, R. E. Stratmann, O. Yazyev, A. J. Austin, R. Cammi, C. Pomelli, J. W. Ochterski, P. Y. Ayala, K. Morokuma, G. A. Voth, P. Salvador, J. J. Dannenberg, V. G. Zakrzewski, S. Dapprich, A. D. Daniels, M. C. Strain, O. Farkas, D. K. Malick, A. D. Rabuck, K. Raghavachari, J. B. Foresman, J. V. Ortiz, Q. Cui, A. G. Baboul, S. Clifford, J. Cioslowski, B. B. Stefanov, G. Liu, A. Liashenko, P. Piskorz, I. Komaromi, R. L. Martin, D. J. Fox, T. Keith, M. A. Al-Laham, C. Y. Peng, A. Nanayakkara, M. Challacombe, P. M. W. Gill, B. Johnson, W. Chen, M. W. Wong, C. Gonzalez, J. A. Pople, *GAUSSIAN 98*, Gaussian Inc., Pittsburgh (PA), 1998.
11. L. Noodleman, J. G. Jr. Norman, *J. Chem. Phys.*, 1979, **70**, 4903.
12. L. Noodleman, *J. Chem. Phys.*, 1981, **74**, 5737.
13. L. Noodleman, E. R. Davidson, *Chem. Phys.*, 1986, **109**, 131.
14. L. Noodleman, D. A. Case, *Adv. Inorg. Chem.*, 1992, **38**, 423.

15. R. Caballol, O. Castell, F. Illas, P. R. Moreira, J. P. Malrieu, *J. Phys. Chem. A*, 1997, **101**, 7860.
16. E. Ruiz, J. Cano, S. Alvarez, P. Alemany, *J. Comp. Chem.*, 1999, **20**, 1391.
17. T. Soda, Y. Kitagawa, T. Onishi, Y. Takano, Y. Shigeta, H. Nagao, Y. Yoshioka, K. Yamaguchi, *Chem. Phys. Lett.*, 2000, **319**, 223.
18. M. Shoji, K. Koizumi, Y. Kitagawa, T. Kawakami, S. Yamanaka, M. Okumura, K. Yamaguchi, *Chem. Phys. Lett.*, 2006, **432**, 343.
19. E. Ruiz, A. Rodriguez-Fortea, J. Cano, S. Alvarez, P. Alemany, *J. Comp. Chem.*, 2003, **24**, 982.
20. A. Bencini, F. Totti, *Int. J. Quantum Chem.*, 2005, **101**, 819.
21. E. M. Zueva, S. A. Borshch, M. M. Petrova, H. Chermette, An. M. Kuznetsov, *Eur. J. Inorg. Chem.*, 2007, 4317.
22. R. Seeger, J. A. Pople, *J. Chem. Phys.*, 1977, **66**, 3045.
23. A. Schafer, C. Huber, R. Ahlrichs, *J. Chem. Phys.*, 1994, **100**, 5829.
24. A. Schafer, H. Horn, R. Ahlrichs, *J. Chem. Phys.*, 1992, **97**, 2571.
25. E. Ruiz, P. Alemany, S. Alvarez, J. Cano, *J. Am. Chem. Soc.*, 1997, **119**, 1297.
26. E. Ruiz, P. Alemany, S. Alvarez, J. Cano, *Inorg. Chem.*, 1997, **36**, 3683.
27. E. Ruiz, J. Cano, S. Alvarez, P. Alemany, *J. Am. Chem. Soc.*, 1998, **120**, 11122.
28. E. Ruiz, C. Graaf, P. Alemany, S. Alvarez, *J. Phys. Chem. A*, 2002, **106**, 4938.
29. E. Ruiz, A. Rodriguez-Fortea, P. Alemany, S. Alvarez, *Polyhedron*, 2001, **20**, 1323.
30. E. Ruiz, J. Cano, S. Alvarez, A. Caneschi, D. Gatteschi, *J. Am. Chem. Soc.*, 2003, **125**, 6791.
31. A. Rodriguez-Fortea, P. Alemany, S. Alvarez, E. Ruiz, *Eur. J. Inorg. Chem.*, 2004, 143.
32. P. Ghosh, E. Bill, T. Weyhermuller, F. Neese, K. Wieghardt, *J. Am. Chem. Soc.*, 2003, **125**, 1293.
33. E. M. Zueva, M. M. Petrova, S. A. Borshch, An. M. Kuznetsov, *Izv. Akad. Nauk, Ser. Khim.*, 2008, 2462 [*Russ. Chem. Bull., Int. Ed.*, 2008, **57**, 2513].
34. C. Aronica, G. Chastanet, E. Zueva, S. A. Borshch, J. M. Clemente-Juan, D. Luneau, *J. Am. Chem. Soc.*, 2008, **130**, 2365.
35. I. B. Bersuker, *The Jahn—Teller effect*, Cambridge University Press, Cambridge, 2006, 632 pp.
36. N. F. Stepanov, *Kvantovaya mekhanika i kvantovaya khimiya* [*Quantum Mechanics and Quantum Chemistry*], Mir, Moscow, 2001, 519 pp. (in Russian).

Received February 13, 2009